

Supplementary Data for:

Dually Responsive Aqueous Gels from Thermo- and Light-Sensitive Hydrophilic ABA
Triblock Copolymers

Jeremiah W. Woodcock, Roger A. E. Wright, Xueguang Jiang, Thomas G. O'Lenick, and Bin
Zhao*

Department of Chemistry, University of Tennessee, Knoxville, Tennessee 37996

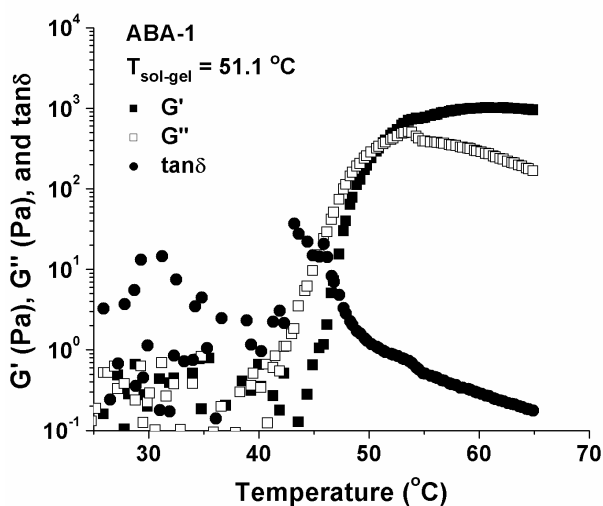


Figure S1. Plot of dynamic storage modulus G' (■), dynamic loss modulus G'' (□), and $\tan\delta$ (●) versus temperature for a 10.0 wt % aqueous solution of PTEGEA-*b*-PEO-*b*-PTEGEA (**ABA-1** in Table 1) in a heating ramp. The rheological data were collected using a heating rate of 3 °C/min, a strain amplitude of 0.2 %, and an oscillation frequency of 1 Hz.

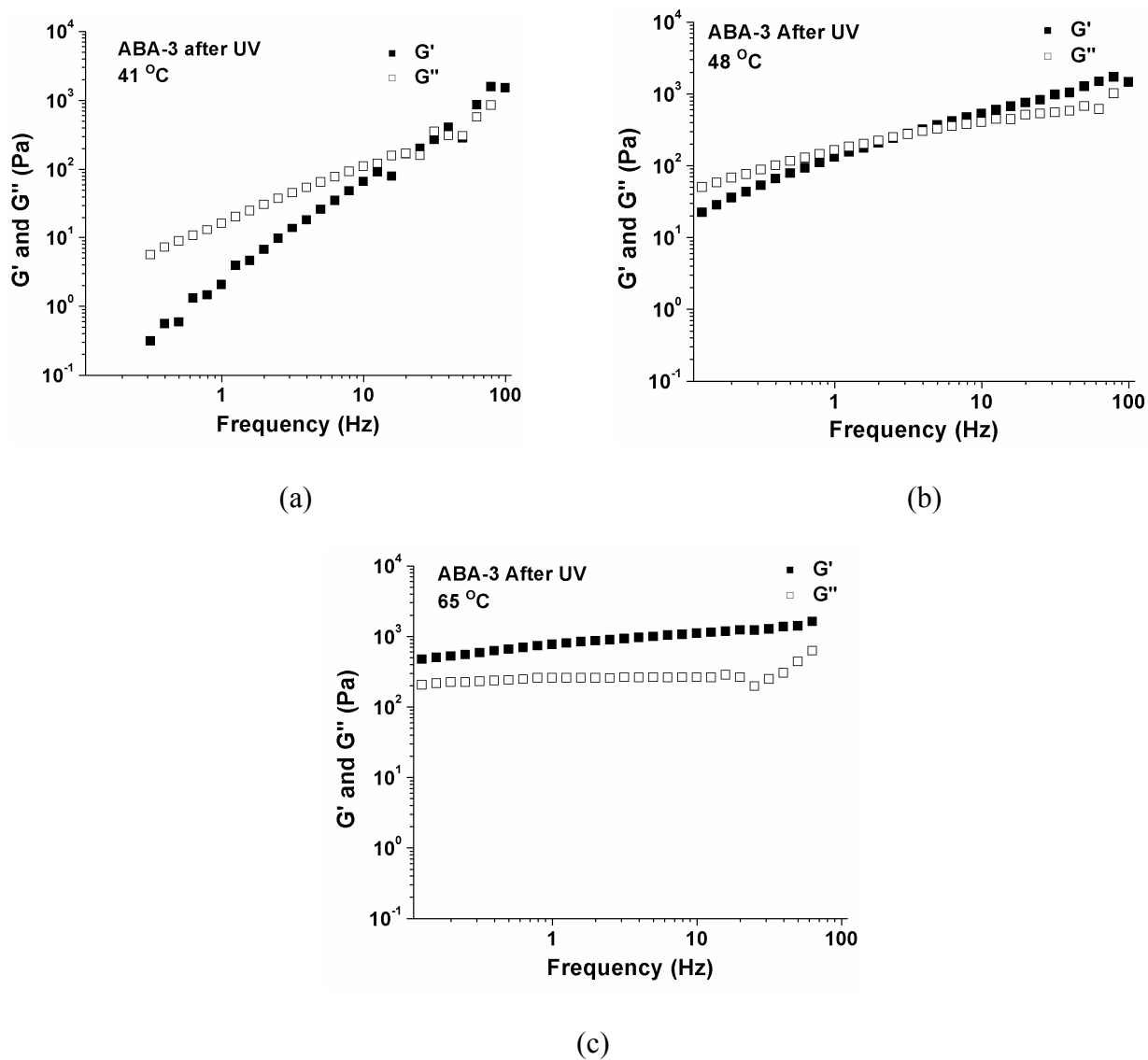
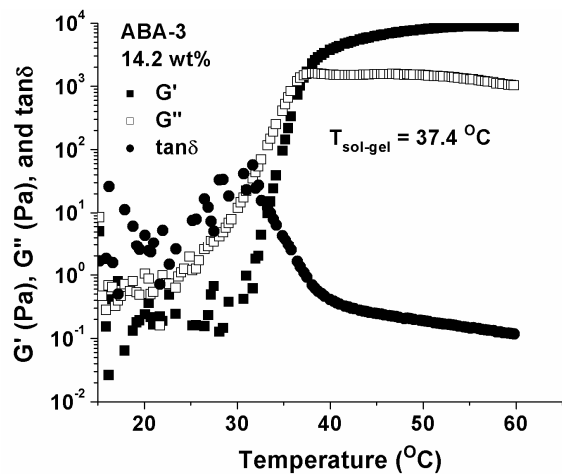
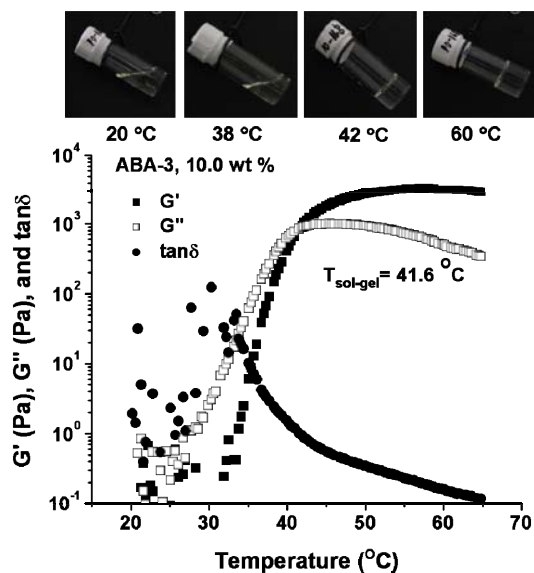


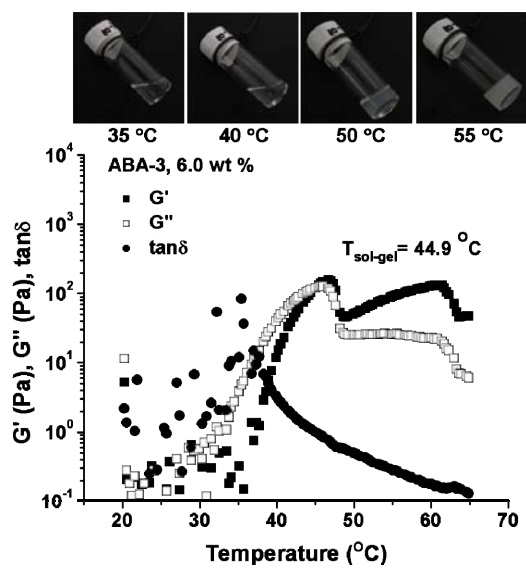
Figure S2. Frequency dependencies of dynamic storage modulus G' (■) and loss modulus G'' (□) of a 9.7 wt % aqueous solution of P(TEGEA-*co*-AA)-*b*-PEO-*b*-P(TEGEA-*co*-AA), obtained from UV irradiation of a 10.0 wt % aqueous solution of P(TEGEA-*co*-NBA)-*b*-PEO-*b*-P(TEGEA-*co*-NBA) (**ABA-3**) at 43 °C for 116 h, at (a) 41, (b) 48, and (c) 65 °C. A strain amplitude of 0.2 % was used in the frequency sweep experiments.



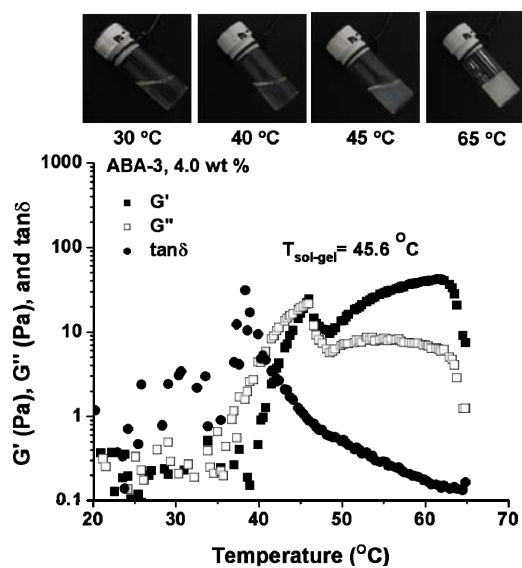
(a)



(b)



(c)



(d)

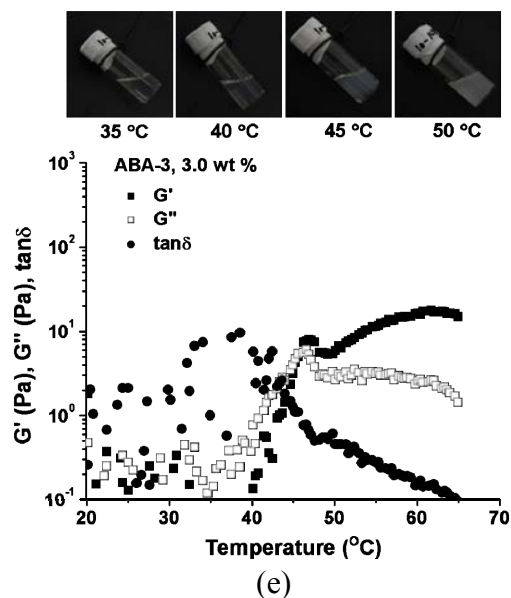


Figure S3. Temperature ramps for aqueous solutions of P(TEGEEA-*co*-NBA)-*b*-PEO-*b*-P(TEGEEA-*co*-NBA) (ABA-3 in Table 1) with concentrations of (a) 14.2, (b) 10.0, (c) 6.0, (d) 4.0, and (e) 3.0 wt %. The rheological data were collected at a constant frequency of 1 Hz, a strain amplitude of 0.2 %, and a heating rate of 3 °C/min. The pictures show the states of each solution at four different temperatures.

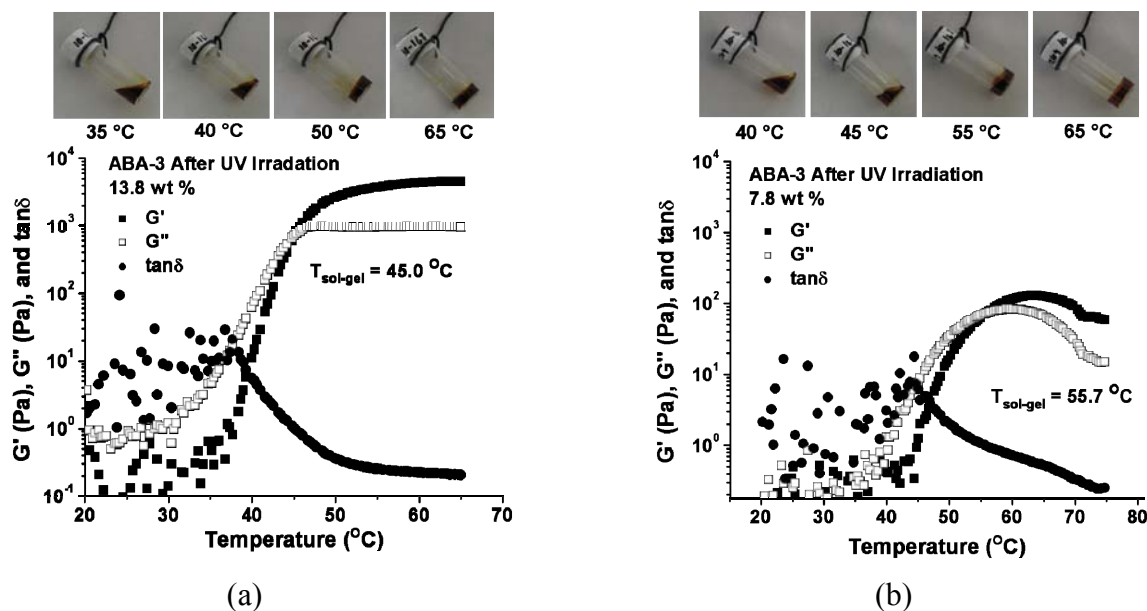


Figure S4. Temperature ramps for aqueous solutions of P(TEGEEA-*co*-AA)-*b*-PEO-*b*-P(TEGEEA-*co*-AA) (obtained from UV irradiation of a 10.0 wt % aqueous solution of ABA-3) with concentrations of (a) 13.8 and (b) 7.8 wt %. The rheological data were collected at a constant frequency of 1 Hz, a strain amplitude of 0.2 %, and a heating rate of 3 °C/min. The pictures show the states of each solution at four different temperatures.



Figure S5. Phase diagram of aqueous solution of P(TEGEA-*co*-NBA)-*b*-PEO-*b*-P(TEGEA-*co*-NBA) (**ABA-3**). !: Sol-gel transition temperature determined by rheological measurements; ,: temperature at which the gel became cloudy, determined by visual examination; 7: temperature at which a clear solution turned cloudy, determined by visual examination.

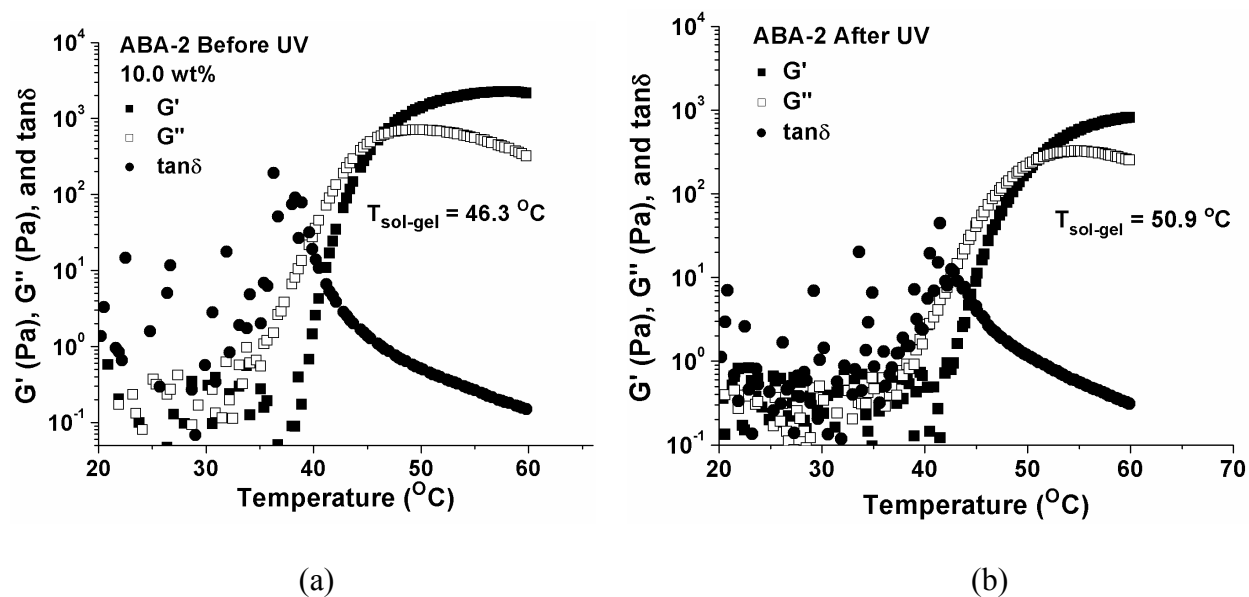


Figure S6. Plot of dynamic storage modulus G' (■), dynamic loss modulus G'' (□), and $\tan\delta$ (●) versus temperature for a 10.0 wt % aqueous solution of P(TEGEA-*co*-NBA)-*b*-PEO-*b*-P(TEGEA-*co*-NBA) (**ABA-2**) before (a) and after (b) the removal of *o*-nitrobenzyl groups. The rheological data were collected from heating ramps using a heating rate of 3 °C/min, a strain amplitude of 0.2 %, and an oscillation frequency of 1 Hz.

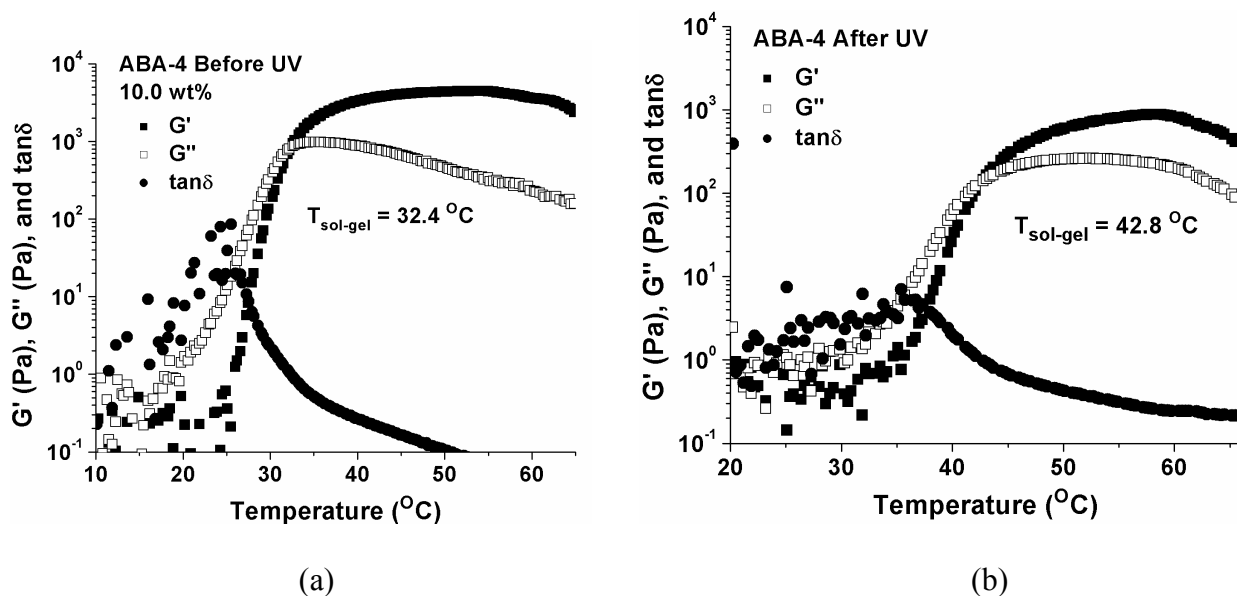


Figure S7. Plot of dynamic storage modulus G' (\blacksquare), dynamic loss modulus G'' (\square), and $\tan\delta$ (\bullet) versus temperature for a 10.0 wt % aqueous solution of P(TEGEA-co-NBA)-*b*-PEO-*b*-P(TEGEA-co-NBA) (ABA-4) before (a) and after (b) the removal of *o*-nitrobenzyl groups. The rheological data were collected from heating ramps using a heating rate of 3 $^{\circ}\text{C}/\text{min}$, a strain amplitude of 0.2 %, and an oscillation frequency of 1 Hz.

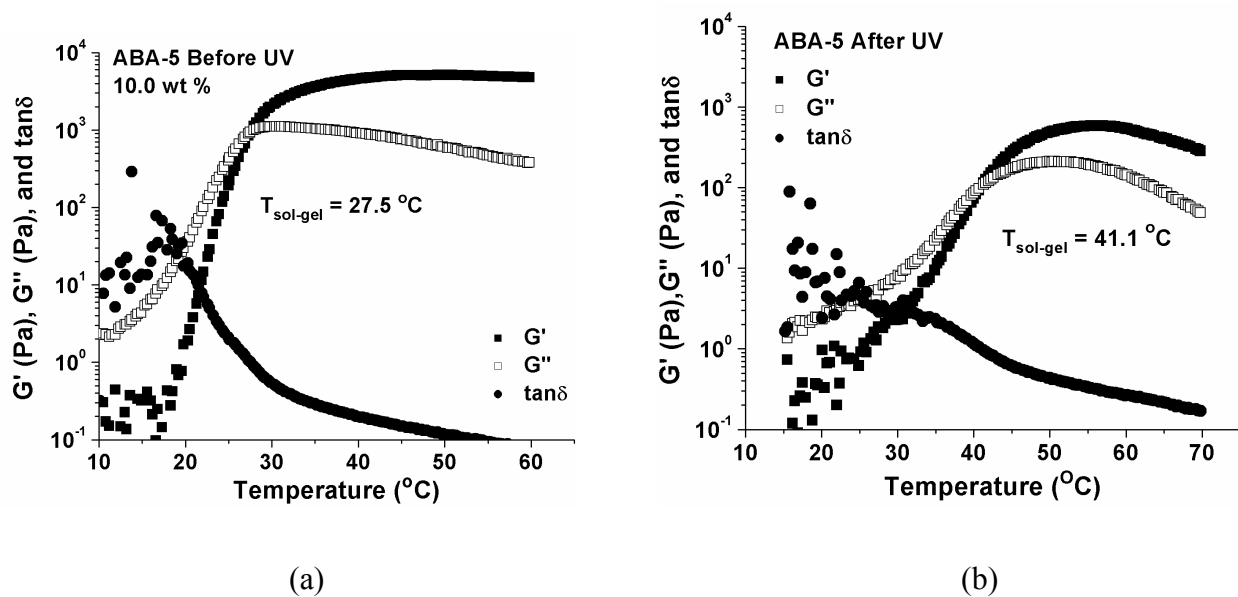


Figure S8. Plot of dynamic storage modulus G' (\blacksquare), dynamic loss modulus G'' (\square), and $\tan\delta$ (\bullet) versus temperature for a 10.0 wt % aqueous solution of P(TEGEA-co-NBA)-*b*-PEO-*b*-P(TEGEA-co-NBA) (ABA-5) before (a) and after (b) the removal of *o*-nitrobenzyl groups. The rheological data were collected from heating ramps using a heating rate of 3 $^{\circ}\text{C}/\text{min}$, a strain amplitude of 0.2 %, and an oscillation frequency of 1 Hz.